01

About the force of electrostatic interaction between two spheroidal macroparticles in the Poisson–Boltzmann model

© S.I. Grashchenkov

Pskov State University,
180000 Pskov, Russia
e-mail: grasi@mail.ru

Received May 26, 2022
Revised August 23, 2022
Accepted August 24, 2022

Electrostatic interaction of two charged spheroidal macroparticles is analyzed within the linearized Poisson–Botzmann model.Interparticle forces are calculated through finite-element method in the regimes of weak and moderate screening with constant surface potentials in the absence of external field.

Keywords: linearized Poisson-Botzmann model, two charged macroparticles, spheroidal macroparticles, colloidal particles, dusty plasmas.

DOI: 10.21883/TP.2022.12.55186.145-22

Introduction

When studying various processes in dusty plasmas and electrolytes, an important role is played by taking into account the forces of electrostatic interaction of charged macroparticles [1,2]. If the potentials of the electric field at the considered points of the plasma or electrolyte are rather small, so that the potential energy of free charge carriers in the electrostatic field is much less than the energy of their thermal motion [2,3], the distributions of φ potential in the vicinity of the particles can be searched based on the linearized Poisson–Boltzmann equation:

$$\Delta\varphi - k_D^2\varphi = 0, \qquad (1)$$

where k_D is screening constant (inverse Debye radius) [4]. A large number of papers relate to forces calculations of the electrostatic interaction of macroparticles based on equation (1), however, if we exclude the asymptotic cases of very small and very large distances between the surfaces of particles [5], they consider the interaction of spherical particles. Usually, in this case, the analysis is carried out on the basis of the solution of equation (1) found in the paper [6]. This solution describes the axially symmetric potential distribution in the vicinity of spherical particles and is represented as infinite series based on the products of Legendre polynomials and modified Bessel functions. A detailed review of these works is given in [7]. Therefore, it is of interest to calculate the force of the electrostatic interaction of particles whose shape differs from spherical. In this paper, using the finite element method, we consider the electrostatic interaction of two charged spheroidal macroparticles with a common axis of symmetry. Note that the distribution of potentials on the surface of particles depends on the distance between them, their sizes, velocities, and the characteristic relaxation time of the surface charge [8], and the search for such a distribution is a separate problem. Therefore, when calculating the interaction forces, one often confines oneself to two limiting cases: a constant surface charge of particles and a constant potential on their surfaces. The latter case takes place at thermodynamic equilibrium in equilibrium plasma and electrolytes [8] and it is this case that will be considered in this paper.

1. Calculation procedure

As already mentioned, in this paper, the finite element method is used to study the electrostatic interaction of macroparticles. In this method the area, in which the distribution of one or another quantity is determined, is divided into a set of subareas. As a result, a computational grid is obtained, on the basis of which a set of basis functions is generated that are used to approximate the desired distribution. Thus, the distribution is sought in the form of expansions into series by these functions with unknown coefficients. At present, there are a number of computer programs that allow to use the finite element method to find a numerical solution of the differential equation by its weak form. Weak form of the equation (1) is [9]:

$$\int_{\Omega}^{\square} \tilde{\nabla} u \tilde{\nabla} \phi d\tilde{V} + \int_{\Omega}^{\square} k^2 u \phi d\tilde{V} = 0, \qquad (2)$$

where

$$u = \frac{\varphi}{\varphi_0}, \quad k = k_D R_1.$$

Here φ_0 is the particle surface potential, Ω is the finite region in which the potential distribution is determined, V is the volume of this region, ϕ is test function. Sequential substitution of test functions into equation (2) makes it possible to obtain a system of equations for calculating the above unknown coefficients. Here and below, the use of a tilde over operators and quantities expressed by

coordinates indicates that the coordinates are normalized to the characteristic size R_1 of the first particle, which in the case of a spherical particle is equal to its radius, and in the case of a spheroidal particle — to the maximum distance from the particle symmetry axis to its surface. We will assume that the corresponding distance R_2 for the second particle does not exceed R_1. Note that the weak form (2) has a unique solution provided that the distribution u is given on the boundary of the region under consideration, or provided that this distribution is given at least on a part of this boundary, and on the rest portion the normal component $\tilde{\nabla}u$ is equal to zero. If the desired distributions are axisymmetric, as in this case, the requirements for computing resources can be reduced by many times passing to cylindrical coordinates, and as a result the three-dimensional problem can be reduced to a two-dimensional one, in which all distributions depend on the polar radius ρ and applicate z of a cylindrical coordinate system only. The information necessary for the transition to a cylindrical coordinate system is given in [10]. With an uniform distribution of the potential on the particle surface, the distribution of the electric field strength **E** on it will coincide with the distribution on the surface of the metal particle. Therefore, the force **F** acting on the particle can be calculated as the force acting on a conductor in a liquid or gaseous dielectric [11]:

$$\mathbf{F} = -\frac{\varepsilon\varepsilon_0}{2}\oint\limits_S^{\square} E^2\mathbf{n}dS. \qquad (3)$$

Here **n** is unit normal vector to the surface element directed inside the body, S is body surface area, ε_0 is electrical constant, ε is permittivity of the medium. From a formal point of view, to solve the problem under consideration it is sufficient to perform calculations according to formulas (2), (3) using any mathematical package supporting the finite element method. However, without special measures aimed at the accuracy improvement of calculations and estimates of the indicated accuracy, the calculations based on the available packages will be incorrect. Let's explain what has been said. The finite element method is inherently approximate method. Therefore, due to calculation errors the resulting potential distribution fluctuates around some true distribution. When calculating surface integrals of functions containing these distributions, the effect of these fluctuations accumulates, and the values of such integrals can be calculated with a significant error. In our case, this leads to a noticeable accuracy decreasing of force calculation by formula (3) in a situation where the change in the field strength along the body surface is small compared to its average value. As a result, the larger k and the distance between macroparticles are, the lower the accuracy of calculations is. Therefore, it is necessary to use additional methods aimed at improving the accuracy of calculations, and to carry out test calculations to evaluate this accuracy. Since the change of the field strength along the surface of the body decreases with distance increasing between the surfaces of particles, then actually the corresponding test calculations are necessary to determine the limiting distances between particles for certain values of k, at which calculations can be performed with the required accuracy.

Let us first consider the methods that were applied to increase the accuracy of calculations. One such method is the use of high order element. It uses hierarchical basis functions [12]. The functions associated with the vertices of the computational grid are linear functions of the barycentric coordinates [13], the value of each of which is equal to unit at one of the nodes and zero at all the others. The functions associated with edges are basis functions, each of which is equal to zero at all vertices and on two edges, and is described by polynomials of some order. The functions associated with cells are equal to zero at the cell boundary and are described using polynomials of some order. A more complete description of these functions can be found in the papers [12,13]. Increasing the order of the basis functions makes it possible to approximate the potential with a smaller number of larger grid cells. In this paper, we assume that such an approach will make it possible to reduce fluctuations of the potential gradient, and thereby increase the accuracy of calculating the forces acting on bodies. One of the packages, supporting work with finite elements of high powers, is the freely distributed package NGSolve [13,14], which is used in this paper. Unfortunately, clear criteria for choosing the optimal orders of basis functions for solving the problem under consideration are unknown, therefore, in this paper we used a simple selection of these orders. As a result, the calculation was performed using polynomials of the fourth power associated with the cells of the computational grid and functions associated with the edges of the tenth power. The NGSolve package is a set of libraries created using the C++ language, designed to build the corresponding basic functions that can be accessed from scripts written in the Python language. For this a module called ngsolve is used. The netgen module is used to build grids. As a result, it is possible to fully describe the required calculation procedure in the Python language. Relevant documentation, including the methods of these modules installation in various operating systems, is available on the website ngsolve.org, and the source codes are contained in the repository https://github.com/NGSolve/ngsolve. Another method for increasing the accuracy of calculations is h-adaptation. h-adaptation is understood as an iterative process of changing the computational grid, leading to a refinement of the desired result. In the simplest case, which is considered in this paper, based on the value of some parameter η calculated for each cell on the basis of the obtained solution, a decision is made to split this cell into two. Note that h-adaptation will not necessarily lead to a monotonous increasing of the force calculation accuracy with the number of cells increasing, since the situation is quite typical when, starting from a certain moment, with the cell size decreasing, the maximum deviations of the

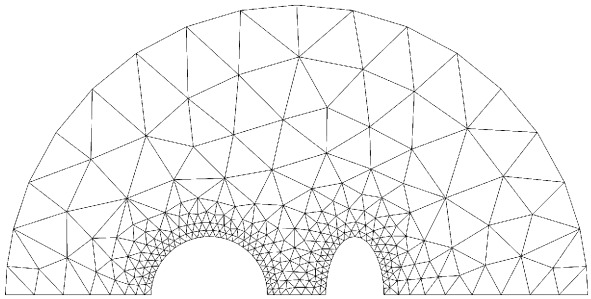

Figure 1. Structure of the initial computational domain.

potential from the true value will decrease, and the gradient deviations increase. As a result, the accuracy of calculating expressions that use integrals of the potential gradient begins to fall. Therefore, *h*-adaptation must be carried out using one or another method for estimating the accuracy of calculations. Before proceeding to the description of the *h*-adaptation method used, let us describe the computational grids used. The NGSolve package allows splitting a two-dimensional computational domain into triangular cells using the Delaunay–Voronoi algorithm [15], based on the size of the edges of these cells on the boundary of the specified domain. An example of the initial computational grid is shown in Fig. 1. The lower boundary of the domain corresponds to the axis of symmetry of the problem.

For the convenience of displaying individual elements, the ratio of their sizes differ from those actually used. The outer boundary radius was assumed equal to $100R_1$ if the distance h_c between macroparticle centers is less than $10R_1$, and $10h_c$ otherwise. On the boundary coinciding with the axis of symmetry, no explicit conditions were specified, since the transition to a cylindrical coordinate system automatically introduces the condition that the radial component of the gradient of the calculated value is equal to zero at $\rho = 0$ [10]. In our case, this means the implicit introduction of the condition that the radial normal component of the potential gradient on the axis of symmetry of the problem is equal to zero. On the outer boundary the potential was initially assumed to be zero and refined in the process of *h*-adaptation by a way that will be described below. The parameter η for each cell was calculated using the following expression [16]:

$$\eta_k = \int\limits_{\Omega_k}^{\square} E^2 dV \int\limits_{\Omega_k}^{\square} (\mathbf{E} - \mathbf{E}_e)^2 dV.$$

Here η_k is a parameter, the value of which is used to judge the need to split the k-th cell, Ω_k is the domain obtained by rotating the k-th two-dimensional cell grid around the symmetry axis of the body, V is its volume. The desired distribution $\mathbf{E}$ of the electric field strength was obtained from the found distribution of potentials. $\mathbf{E}_e$ distribution was obtained by extrapolation of the obtained distribution $\mathbf{E}$ using vector basis functions. To extrapolate the distribution $\mathbf{E}$, we used the set of basis functions described in the papers [13,14] that make up the Sobolev space H^1, and to extrapolate the distribution $\mathbf{E}_e$ the set of basis functions described in the paper [13] that make up the space $H(\mathrm{div})$. The notations used here for functional spaces coincides with those generally accepted in the literature for finite elements and with the notations in papers [13,14], where one can find their detailed description. The orders of the corresponding types of basis functions related to different spaces were assumed to be the same. At each iteration step, the splitting was carried out for those cells for which the condition $\eta_k > 0.5\eta_{\max}$ was satisfied, where $\eta_{\max}$ is the maximum value η_k. At distances from the outer boundary less than 0.2 of its radius the *h*-adaptation was not carried out, and the values of the parameter η_k for the corresponding cells were not considered when finding $\eta_{\max}$. The nature of the grid change during *h*-adaptation is illustrated in Fig. 2. The adaptation process is repeated until the number of degrees of freedom, understood in this case as the total number of unknowns in the expansion of the desired solution by the basis functions, does not exceed 10^6. From a formal point of view, the zero potential at the outer boundary means that, from a physical point of view the boundary is represented by a conductor on which induced charges are induced that act on particles. This effect decreases with the increasing of size of the considered domain and of k value. It is possible to reduce the size of the domain without reducing the calculation accuracy if the potential at the outer boundary is set at least on the basis of some approximate solution. In the present paper, in the process of grid adaptation the particle charges are calculated at each step using the Gauss theorem. Further, the potential distribution at the outer boundary is approximately represented as a distribution obtained by a superposition of distributions created by single spherical macroparticles [1], whose position coincides with the centers of the considered macroparticles, and the charges coincide with those found at the previous step. Note that such refinement of the potential at the outer boundary makes it possible to obtain a noticeable accuracy increasing of calculations or size decreasing of the computational domain at a given accuracy only for k values that differ from zero by maximum a few hundredths. For

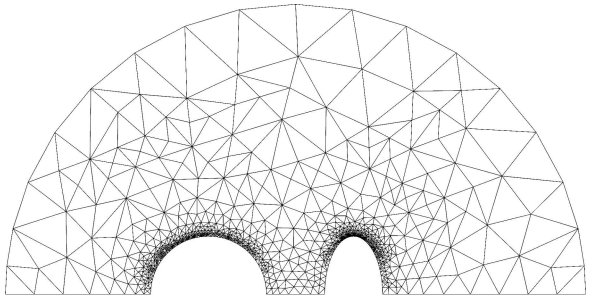

Figure 2. Computational domain after several steps of *h*-adaptation.

large k, due to a faster potential decreasing with distance from the particles, such refinement becomes irrelevant. Using the described algorithm, the time for calculating the force of interaction between macroparticles using Intel(R) Core(TM) i9-10980XE processor was, depending on the situation under consideration, from 5 to 9 min.

Let us now describe the test calculations performed. As the distance h between the surfaces of spherical macroparticles increases, the force F of their electrostatic interaction tends to the repulsive force F_{DLVO}, described by the asymptotic expression [8]

$$F_{\mathrm{DLVO}} = F_0 4\pi \frac{R_2}{R_1} \frac{1+\tilde{h}_c k}{\tilde{h}_c^2} \exp(-k\tilde{h}),$$

where

$$F_0 = \varepsilon\varepsilon_0\varphi_0^2.$$

For identical particles at $k = 1$, $\tilde{h} = 5$, the difference between the force modules acting on the first and second macroparticles, which occurs due to inaccurate calculations, was 0.13%, and the difference of the average value of these modules from F_{DLVO} was 0.1%. For the same k and $\tilde{h}$, if the radius of the second particle by two times was lower the radius of the first particle, these differences were 0.048 and 0.044%, respectively. In paper [17] using the same approach as in the papers [6,8], the dependence of the electrostatic repulsion force of spherical particles at a given potential on their surfaces on the distance between these surfaces at $k = 1$ was plotted. With the accuracy, which can be judged from the graphically presented data, the results of calculations carried out for $\tilde{h}$ from 0.01 to 4 on the basis of the presented method coincided with the results of the paper [17]. In the paper [8] the dependence of the electrostatic repulsion force of spherical particles at a given potential on their surfaces on the distance between these surfaces was plotted for $k = 0.12$ and $\tilde{h}$ values from 1.5 to 15. Based on the method developed in this paper, the same dependence was plotted. The resulting curve coincided with the curve given in the paper [8]. Note that, with the unchanged allocated computing resources, the achievable accuracy of calculations based on all solutions obtained using the approach of work [6] decreases with k and $\tilde{h}$ decreasing, while the accuracy of calculations based on method proposed in this paper increases. In the paper [18], using a bispherical coordinate system, based on the Laplace equation, expressions were obtained that allow one to calculate the interaction forces of charged unshielded metal balls for given charges of these particles. These expressions were used for test calculations at $k = 0$. In the calculations based on the expressions obtained in [18], the charge values obtained in the process of grid adaptation were used. Calculations carried out for particles of identical radii showed that at $\tilde{h} = 20$ the difference between the force modules acting on the first and second macroparticles, which arises due to inaccurate calculations, was 0.17%, and between the average of these forces and the force obtained by expressions in paper [18], — 0.11%. And if the radius of the second particle by two times was lower the radius of the first particle, these differences were 0.016 and 0.008%, respectively. To illustrate the accuracy increasing with distance decreasing between the surfaces of macroparticles, we state that for two particles of equal radius at $\tilde{h} = 0.01$, the difference between the force values obtained on the basis of the proposed method and the expressions of the paper [18] was 0.0002%.

Thus, we see that the developed method of calculation is quite applicable for finding the forces of electrostatic repulsion of macroparticles at not too large distances between their surfaces and $k \leq 1$, and the difference between the modules of the forces acting on the first and second macroparticles can serve as the upper limit of the possible calculation errors.

2. Study of macroparticles shape for the strength of their electrostatic interaction

The developed calculation algorithm was applied to study the interaction of spheroidal particles at different values of the screening constant. Fig. 3 shows the forces acting on spheroidal particles vs. minimum distance between their surfaces at $k = 1$ and $R_1 = R_2$. The values a_1 and a_2 in the text to the Figure represent, respectively, for the first and second macroparticles the distances from the center of the particle to its surface along the axis connecting the centers of the particles. It can be seen from this Figure that for particles with the same cross-section and a sufficient degree of their screening the decreasing of the longitudinal dimensions of the particles leads to increasing of their electrostatic repulsion forces, and these sizes increasing — to these forces decreasing. However, as can be seen from Fig. 4, which shows the same dependences, but at $k = 0.1$, if the screening degree is

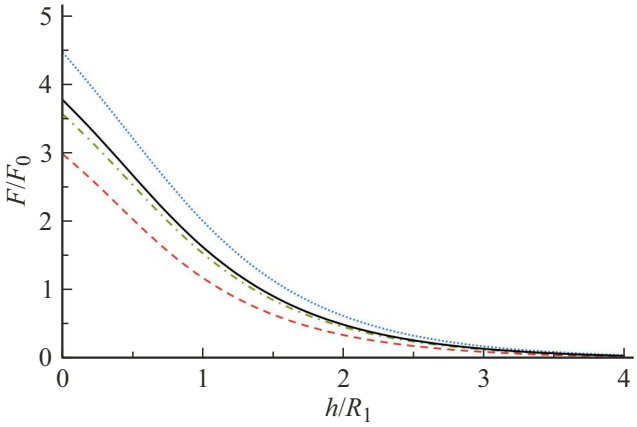

Figure 3. Normalized force vs. normalized distance between particle surfaces for $k = 1$ and $R_1 = R_2$: dotted line — $a_1/R_1 = a_2/R_2 = 0.5$; solid — balls of equal radius; dash-dotted line — $a_1/R_1 = 2$, $a_2/R_2 = 0.5$; dashed — $a_1/R_1 = a_2/R_2 = 2$.

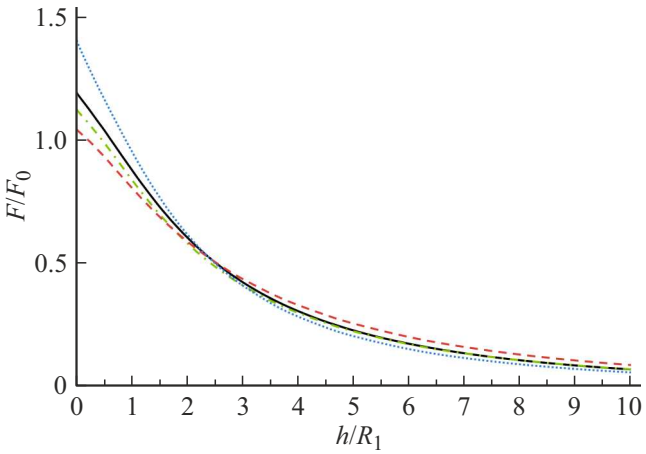

Figure 4. Normalized force vs. normalized distance between particle surfaces for $k = 0.1$ and $R_1 = R_2$: dotted line — $a_1/R_1 = a_2/R_2 = 0.5$; solid — balls of equal radius; dash-dotted line — $a_1/R_1 = 2$, $a_2/R_2 = 0.5$; dashed — $a_1/R_1 = a_2/R_2 = 2$.

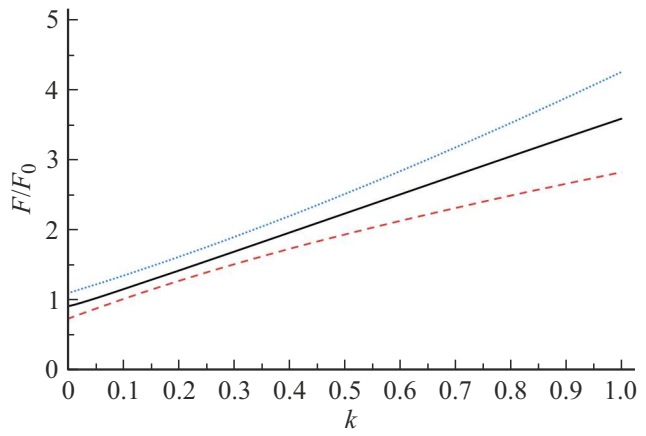

Figure 5. Normalized force vs. normalized screening constant for $h/R_1 = 0.1$ and $R_1 = R_2$: dotted line — $a_1/R_1 = a_2/R_2 = 0.5$; solid — balls of equal radius; dashed — $a_1/R_1 = a_2/R_2 = 2$.

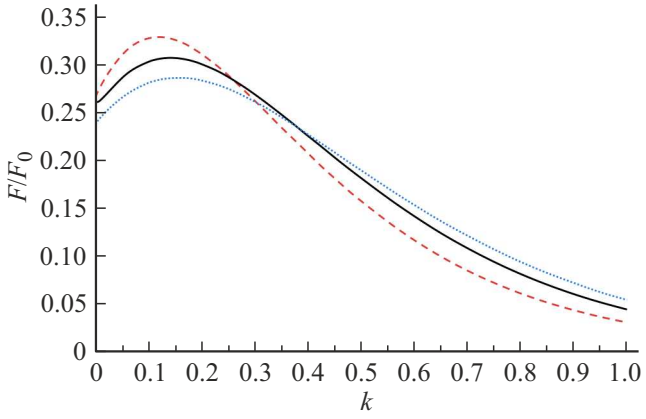

Figure 6. Normalized force vs. normalized screening constant for $h/R_1 = 4$ and $R_1 = R_2$: dotted line — $a_1/R_1 = a_2/R_2 = 0.5$; solid — balls of equal radius; dashed — $a_1/R_1 = a_2/R_2 = 2$.

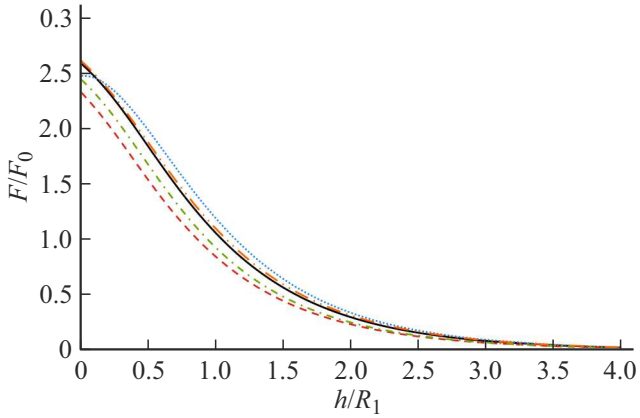

Figure 7. Normalized force vs. normalized distance between particle surfaces at $k = 1$ and $R_1 = 2R_2$: dotted line — $a_1/R_1 = a_2/R_2 = 0.5$; long stroke — double dotted line — $a_1/R_1 = 0.5$, $a_2/R_2 = 2$; solid line — balls; dash-dotted — $a_1/R_1 = 2$, $a_2/R_2 = 0.5$; dashed — $a_1/R_1 = a_2/R_2 = 2$.

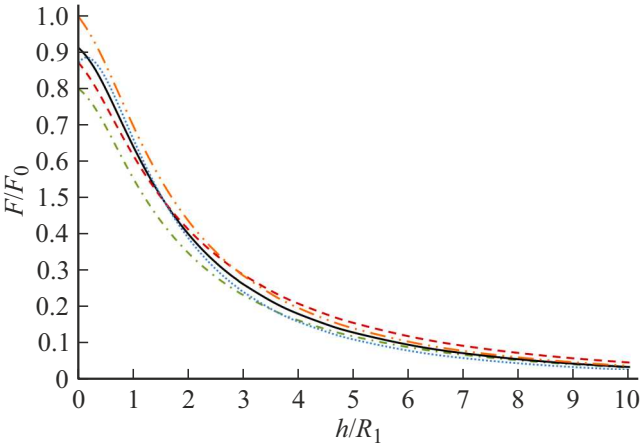

Figure 8. Normalized force vs. normalized distance between particle surfaces at $k = 0.1$ and $R_1 = 2R_2$: dotted line — $a_1/R_1 = a_2/R_2 = 0.5$; long stroke — double dotted line — $a_1/R_1 = 0.5$, $a_2/R_2 = 2$; solid line — balls; dash-dotted — $a_1/R_1 = 2$, $a_2/R_2 = 0.5$; dashed — $a_1/R_1 = a_2/R_2 = 2$.

not large enough, then such dependence of the force on the longitudinal size of the particle is observed only up to a certain distance between the surfaces of macroparticles. The aforesaid is additionally illustrated in Figs 5 and 6, from which it is seen that at a sufficiently large distance between the surfaces of macroparticles, depending on the degree of screening the interaction force of macroparticles can increase both upon increasing and decreasing of their longitudinal dimensions. Moreover, a situation is possible when both increasing and decreasing of the longitudinal dimensions of the particles will lead to decreasing of the interaction force between them. Besides, as can be seen from Figs 7, 8, for particles of different lateral dimensions the same situation can also arise at small distances between their surfaces.

Conclusion

The electrostatic interaction of two charged spheroidal macroparticles with a common axis of symmetry and a constant potential on their surfaces under conditions of weak and moderate screening is considered. Calculations show that at sufficiently high degree of screening and the same lateral dimensions of particles at a constant distance between their surfaces, the decreasing of their longitudinal dimensions leads to increasing of the forces of electrostatic interaction between them. However, if the degree of screening is not large enough or the lateral dimensions of the particles are different, then there is no such unambiguous dependence of the force on the lateral dimensions of the particles. In this case, at different degrees of screening and the ratio of the lateral dimensions of macroparticles at different distances, the nature of the dependence of the interaction force between particles on their longitudinal dimensions can be different. In this case, a situation is possible when the interaction force between spherical macroparticles will be greater than the interaction forces of particles both in the form of an oblate spheroid and in the form of elongated spheroid.

Conflict of interest

The author declares that he has no conflict of interest.

References

[1] V.E. Fortov, A.G. Khrapak, S.A. Khrapak, V.I. Molotkov, O.F. Petrov. Phys. Usp., **47** (5), 447 (2004). DOI: 10.1070/PU2004v047n05ABEH001689
[2] H. Ohshima. *Theory of Colloid and Interfacial Electric Phenomena* (Academic Press, San Diego, 2006)
[3] G. Ecker. *Theory of Fully Ionized Plasmas* (Academic Press, NY., 2013)
[4] P. Debye, E. Huckel. Phys. Zeitschr., **24** (9), 185 (1923).
[5] J.N. Israelachvili. In: *Intermolecular and Surface Forces* (Elsevier Science, Netherlands, 2011)
[6] S. Marčelja, D.J. Mitchell, B.W. Ninham, M.J. Sculley. J. Chem. Society, Faraday Transactions 2: Molecular Chem. Phys., **73** (5), 630 (1977). DOI: 10.1039/F29777300630
[7] S.V. Siryk, A. Bendandi, A. Diaspro, W. Rocchia. J. Chem. Phys., **155** (11), 114114 (2021). DOI: 10.1063/5.0056120
[8] I.N. Derbenev, A.V. Filippov, A.J. Stace, E. Besley. Soft Matter, **14** (26), 5480 (2018). DOI: 10.1039/c8sm01068d
[9] Z. Chen. *Finite Element Methods and Their Applications*. (Springer, Berlin, Heidelberg, 2010)
[10] J.N. Reddy, D.K. Gartling. *The Finite Element Method in Heat Transfer and Fluid Dynamics* (CRC Press, Boca Raton, 2010)
[11] I.E. Irodov *Osnovnye zakony elektromagnetizma. Ucheb. posobie dlya studentov vuzov. 2 izd. sterotip*. (Vysshaya shkola, M., 1991) (in Russian)
[12] P. Solin, K. Segeth, I. Dolezel. *Higher-Order Finite Element Methods* (Chapman and Hall/CRC, NY., 2003)
[13] S. Zaglmayr. *Phd Thesis* (Johannes Kepler University, Linz, 2006)
[14] J. Schöberl. *„ C++11 Implementation of Finite Elements in NGSolve", ASC Report 30/2014, Institute for Analysis and Scientific Computing* (Vienna University of Technology, Vienna, 2014)
[15] B. Lucquin, O. Pironneau. *Introduction to Scientific Computing* (Wiley, Chichester, 1998) DOI: 10.1023/A:1004355614429
[16] S.I. Grashchenkov. Surf. Engin. Appl. Electrochem., **58** (1), 75 (2022). DOI: 10.3103/S1068375522010033
[17] A.V. Filippov, I.N. Derbenev, A.A. Pautov, M.M. Rodin. J. Experiment. Theor. Phys., **125** (3), 518 (2017). DOI: 10.1134/S1063776117080040
[18] S.I. Grashchenkov. Tech. Phys., **56** (7), 914 (2011). DOI: 10.1134/S1063784211070115